JOURNAL OF MATERIALS SCIENCE 32 (1997) 2937–2947

Sedimentation behaviour of kaolinite and montmorillonite mixed with iron additives, as a function of their zeta potential

A. C. PIERRE*, K. MA
Department of Mining, Metallurgical, and Petroleum Engineering, University of Alberta, Edmonton, Alberta, Canada

In order better to understand the packing structure of clay sediments mixed with iron additives, as observed in a scanning electron microscope and published in previous studies, an experimental investigation of the zeta potential of clay particles was undertaken. The results were used to build sedimentation diagrams comparable with the experimental sedimentation diagrams. The results were analysed in the light of the known behaviour of iron additives in aqueous solutions and their interaction with clay particles.

1. Introduction

In previous publications, we reported on the sedimentation behaviour and the floc structure of montmorillonite and kaolinite sediments in the presence of iron electrolytes [1–3]. It would be interesting to examine the relation between the structure of these flocs and the electrostatic stabilization theory, also known as the Derjaguin, Landau, Verwey and Overbeek theory (DLVO theory). In the present study, a partial attempt in this direction was carried out by measuring the zeta potential of clay particles and by establishing a correlation between the value of the zeta potential and the type of sediment structure.

2. Experimental procedure

The clays studied were mostly the kaolinite "Hydrite UF" (HUF) from the Georgia Kaolin Company, the montmorillonite "SWy-1" from the Clay Minerals Repository of the Clay Minerals Society at the University of Missouri, and in a few cases the "Hydrite R" (HR) from the Georgia Kaolin Company. The two hydrites had the same composition, as reported by the supplier, but the average particle sizes were different: 0.20 and 0.77 μm, respectively, for the HUF and HR kaolinites. The montmorillonite particle size was of the order of 1 μm, according to scanning electron micrographs. However, they were much thinner (although the micrographs do not make it possible to venture a value) than the kaolinite particles. The montmorillonite specific area was 32 $m^2 g^{-1}$ according to the supplier, by comparison with 21 and 10 $m^2 g^{-1}$ for HUF and HR kaolinites.

HUF and HR kaolinites were converted to the sodium form by the method given by Schofield and Samson [4]. This treatment is supposed to give negative charges to the faces and positive charges to the edges of the kaolinite particles. Next, these kaolinites were treated with a 0.5 M $Na_4P_2O_7$ solution, according to a method given by van Olphen [5] and Yaalon [6]. Such a treatment is known to provide negative charges to both the edges and the faces of kaolinite particles, before mixing with other electrolytes [7]. The objective was to pursue a study on the aggregation of plate-like particles, when a single type of electric charge dominates on both the edges and the faces of the particles.

In a first series of samples, suspensions containing 0.5% (by mass) HUF kaolinite were prepared in graduated cylinders, and the total suspension volume in each cylinder was 100 ml. The pH values were respectively adjusted to 2, 4, 6, with HCl, and to 8, 9.5, 10, and 11 with NaOH. At each pH, the effect of unaged $FeCl_3$ at concentrations of 0.17, 0.33, 0.67, 1.67, and 3.3 mM was studied. "Unaged $FeCl_3$ solution", indicates that the iron electrolyte was dissolved just prior to a clay sedimentation experiment. Other authors called such iron solutions "fresh solutions".

In order to get some insight into the role of Fe^{3+} hydrolysis on the flocculation behaviour of clay, the effect of aged $FeCl_3$ at concentrations of 0.17, 0.33, 0.67, 1.67, 3.3, 5, and 10 mM were examined at the pH values of 2, 4, 6, 9.5, and 11. Aged iron samples were prepared in beakers containing 500 ml 0.5 M solution $FeCl_3$ in distilled water, which were allowed to age for a month. With time, a fine suspension formed in the brown solution. By using atomic absorption spectrophotometry, after centrifugation of the iron suspension, it was found that the iron concentration in the solution had stabilized to a value of ≈ 0.33 M. The aged $FeCl_3$ suspension was agitated before mixing

* *Present address*: Université Claude Bernard-Lyon I, LACE, Bât. 303, 43 Bd. du 11 November 1918, 69622 Villeurbanne Cedex, France.

with the clay suspensions in order to add the desired amount of iron.

The sedimentation of montmorillonite suspensions mixed with aged $FeCl_3$ was also investigated. The montmorillonite content in the suspensions was 1%, and 100 ml clay suspensions samples were prepared. Before adding any electrolyte, the suspension pH was ≈ 9.5. The pH values investigated in the present study were 2, 4, 6, 9.5 and 12 and they were achieved by adding HCl or NaOH to the suspension, depending on the pH. The aged $FeCl_3$ concentrations studied at each pH were 0.33, 1, 2, 3.3, 5 and 10 mM.

Finally, a series of sedimentations was performed by mixing hydroxoferric particles in montmorillonite suspensions. The pH values were the same as before, and the hydroxoferric particles contents were 0.025%, 0.125%, 0.25% and 0.50% (by mass) at each pH. These hydroxoferric particles were made by the method described by Ohtsubo *et al.* [8]. This consists of adding drop by drop a saturated sodium bicarbonate ($NaHCO_3$) solution to a solution of 48.66 g $FeCl_3$ in 300 ml distilled water, until the pH reaches 1.5. Precipitation occurs, and the precipitate was termed amorphous iron hydroxide, ferrihydrite or hydroxoferric particles, depending on the authors. In the present work, the term hydroxoferric particles, as used by Blackmore [9], is adopted. The excess salt was removed from this precipitate by dialysis in distilled water. The distilled water was renewed until the pH of the suspension was in the range 3.8–4.2. The solid content in the suspension was 2.5 g/100 ml.

The packing structure of the sediments, observed in a scanning electron microscope (SEM) after supercritical drying in CO_2, has been reported in previous publications [1, 3]. The experimental data in the present paper focus on the experimental determination of the zeta potential of clay particles, in the electrolyte conditions which were mentioned before, and in trying to relate the sedimentation behaviour to these measured zeta potentials.

Other partial characterizations were made. These include: (1) some measurements by atomic absorption spectroscopy of the iron precipitated with the clay in the wet sediments; (2) some limited observations by transmission electron microscopy (TEM) of the iron compounds which were precipitated with the clay particles; and (3) some limited measurement of the sediment viscosity.

The equipment used to determine the zeta potential of clay particles was a micro-electrophoresis Mark II apparatus (Rank Brothers company). For each data point, the electrophoretic mobilities of a minimum of five particles were successively measured, first when applying the electric field in one direction, then after reversing the polarity of the applied electric field, and an average value was recorded. Because the 0.5% (by mass) kaolinite and the 1% (by mass) montmorillonite suspensions were too dense to measure their zeta potential directly, these clay suspensions were first diluted to 0.05% and 0.01%, respectively, in distilled water. In each case, and just before measuring a zeta potential, the pH was adjusted to the value the suspension had before dilution, with the addition of HCl or NaOH, depending on this pH. In the same way, some iron electrolyte was added to each clay suspension in order to maintain the initial concentration of these electrolytes before dilution.

For the other limited characterizations, in clay suspensions where a clear supernatant liquid naturally formed after 12 h, the iron content in this supernatant liquid was directly analysed by atomic absorption spectroscopy. In clay suspensions where this did not occur, the suspension was centrifuged until a clear supernatant liquid separated from the suspension. These clear liquids were used for chemical analysis. The equipment used was a Perkin–Elmer 4000 AAS atomic absorption spectrophotometer.

For the TEM observations, a diluted suspension was dropped on to a carbon-coated copper grid. Two different TEMs were used in this study: a Philips EM 300 TEM, and a Jeol-2010 analytical TEM. The latter microscope was connected to an X-ray detector, to determine the energy-dispersed X-ray spectrum (EDX).

The rheological properties of a series of montmorillonite–hydroxoferric particles suspensions were determined using a cylindrical rotor viscometer, of the type Contrave Rheomat 115. Flow curves were first recorded and the Bingham yield stress of a suspension was determined from the data at increasing shear rate. The montmorillonite content in the suspensions was 1% by mass. The pH values investigated were 2, 4, 6, 8, 9.5 and 12, while the hydroxoferric contents of the suspensions were 0%, 0.025%, 0.12%, 0.25% and 0.5% (by mass) at each pH.

3. Results

3.1. Sedimentation behaviour and diagrams

Three types of sedimentation behaviour of clay suspensions mixed with iron electrolytes were reported in previous publications. The first type was termed accumulation sedimentation (Fig. 1a). In this regime, individual particles or small aggregates fell and accumulated at the bottom of a beaker. After supercritical drying in CO_2, SEM observations showed that the sediment was composed of a random and roughly uniform packing of clay particles. During sedimentation, a sharp interface separated the accumulated sediment from the remaining clay suspension. This interface moved upwards with time, as more clay particles accumulated. The appearance of an accumulated sediment is illustrated in Fig. 2a.

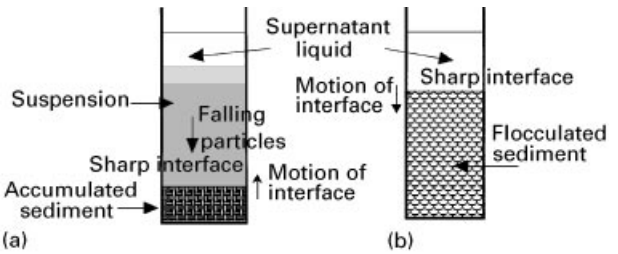

Figure 1 Accumulation and flocculation sedimentation behaviour.

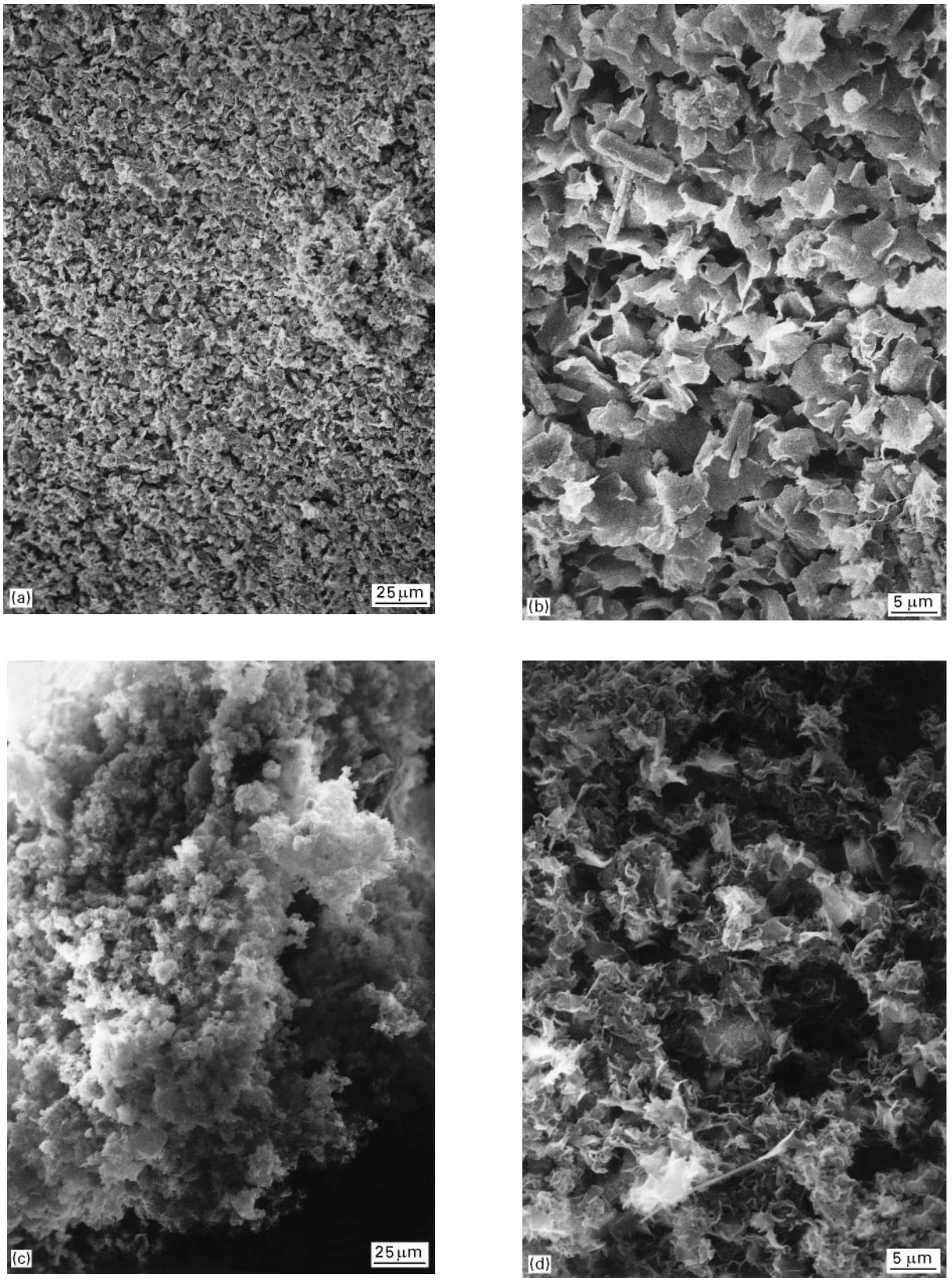

Figure 2 Scanning electron micrographs of 1% montmorillonite suspensions: (a, b) accumulated sediment made at pH = 9.5 without any iron additive; (c, d) flocculated sediment made at pH = 9.5 with 0.5% by mass hydroxoferric particles.

The second type of sedimentation behaviour was termed flocculation sedimentation (Fig. 1b). In this regime, a suspension separated very quickly into a sediment and a clear supernatant liquid on top of the sediment. The sediment was relatively thick and it had a uniform visual appearance. This sediment was much less compact than an accumulated sediment. Its observation by SEM after supercritical drying in CO_2 showed that it was composed of fractal flocs, such as in the aggregates described in the diffusion limited aggregation model (DLA). The separation interface between the flocculated sediment and the supernatant liquid was sharp and it moved downwards with time. That is, the flocculated sediment underwent a slow compacting process with time. Such a floc structure is illustrated in Fig. 2b.

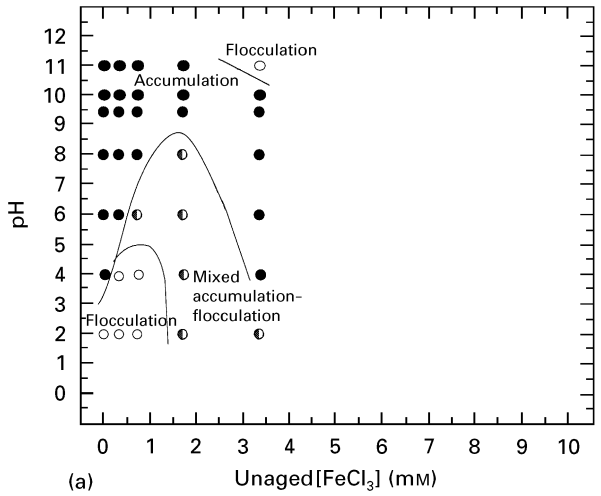

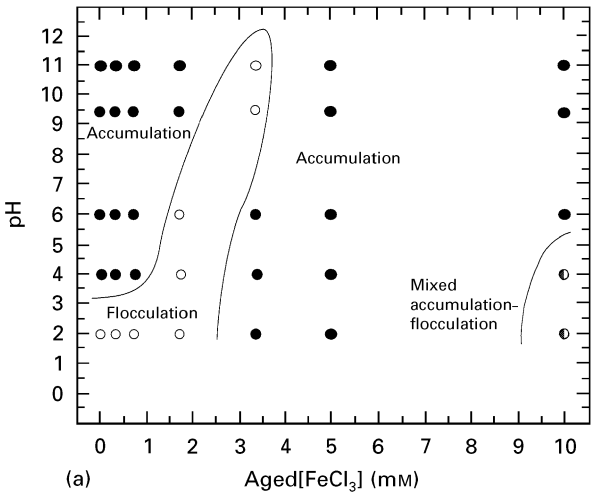

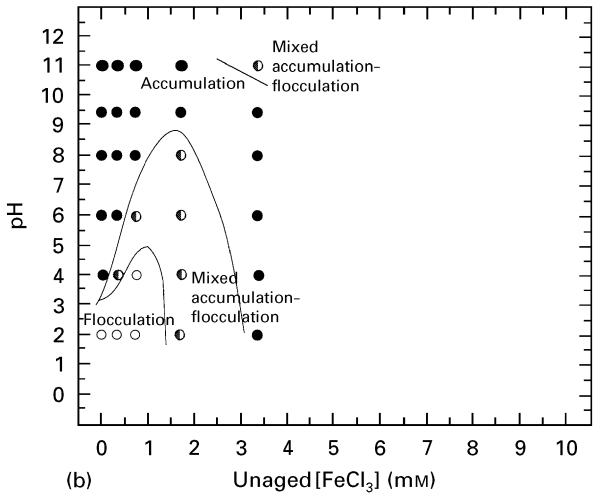

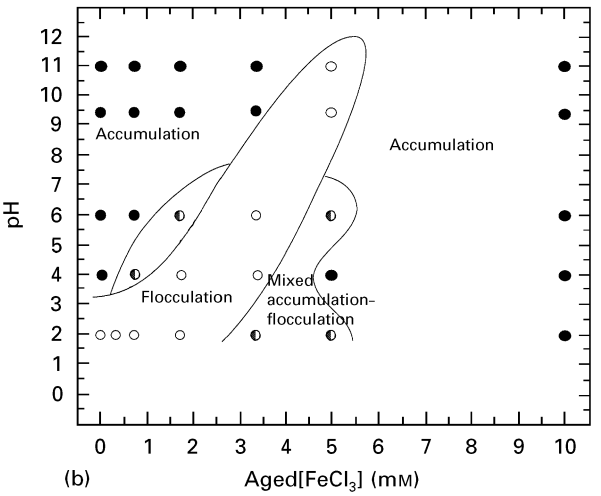

Figure 3 Diagrams of the sedimentation behaviour of 0.5% sodium-kaolinite suspensions treated with $Na_4P_2O_7$ and mixed with unaged $FeCl_3$. (a) Experimental observations: (●) accumulation, (○) flocculation, (◐) mixed behaviour. (b) Predictions from the measured zeta potential ζ: (●) $|\zeta| < 10$ mV, (○) $|\zeta| > 15$ mV, (◐) 10 mV $\leq |\zeta| \leq$ 15 mV.

Figure 4 Diagrams of the sedimentation behaviour in 0.5% sodium-kaolinite suspensions treated with $Na_4P_2O_7$ and mixed with aged $FeCl_3$. (a) Experimental observations: (●) accumulation, (○) flocculation, (◐) mixed behaviour (b) Predictions from the measured zeta potential ζ: (○) $|\zeta| < 10$ mV, (●) $|\zeta| > 15$ mV, (◐) 10 mV $\leq |\zeta| \leq$ 15 mV.

A third type of sedimentation behaviour, termed mixed flocculation–accumulation, involved accumulation in a primary stage, then flocculation of the remaining suspension in a second stage. That is , initially individual particles started to accumulate at the bottom of the beaker. Then, after some time, the remaining clay suspension could flocculate, on top of the accumulated sediment.

These three types of sedimentation behaviour were observed when unaged $FeCl_3$ was added to kaolinite suspensions. A diagram which summarizes the sedimentation behaviour in this system is shown in Fig. 3a, where dotted lines are tentatively drawn to outline the ranges of conditions where each type of sedimentation occurred. The three types of sedimentation behaviour were also observed in kaolinite suspensions mixed with aged $FeCl_3$. The diagram summarizing the sedimentation behaviour of this system is shown in Fig. 4a.

Diagrams were also drawn for the sedimentation behaviour of HUF kaolinite suspensions containing 1%, 2%, and 5% by mass of clay mixed with unaged $FeCl_3$. These diagrams were similar to each other. However, the field where accumulation sedimentation occurred decreased as the clay content increased.

According to an analysis by Michaels and Bolger [10], it is possible to estimate the ratio C_{Fp} between the volume fraction, Φ_F, occupied by the flocs in a suspension, and the volume fraction, Φ_p, occupied by dense kaolinite particles. If the final sediment volumes are V_{F1} and V_{F2} when the dense kaolinite particles volume fractions are Φ_{p1} and Φ_{p2}, in suspensions with the same initial volume, V_0, C_{Fp} is given by

$$C_{Fp} = \frac{0.62}{V_0}\left(\frac{V_{F1} - V_{F2}}{\Phi_{p1} - \Phi_{p2}}\right) \quad (1)$$

From the data on the final sediment thickness of 2% and 5% HUF sodium-kaolinite suspensions, the value of C_{Fp} could be calculated as a function of unaged $FeCl_3$ concentration and pH. The results are reported in Fig. 5, and they show the flocs were from 12–25 times less compact than dense kaolinite particles. The lowest compacting (highest C_{Fp} value) occurred for a $FeCl_3$ concentration of 5 mM, at all pH.

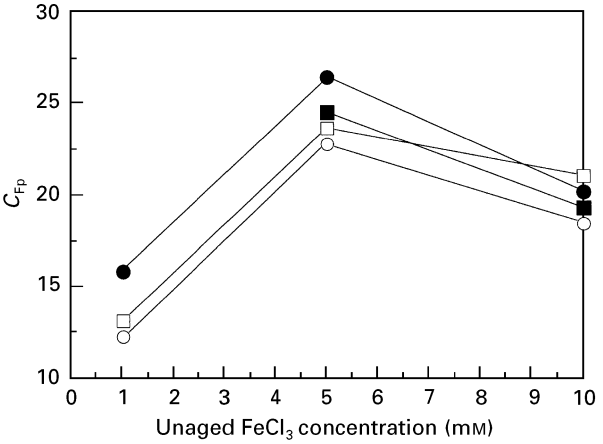

Figure 5 Ratio C_{Fp} between the volume occupied by the flocs and the volume occupied by dense kaolinite particles, in HUF kaolinite suspensions treated with $Na_4P_2O_7$, as a function of the concentration of unaged $FeCl_3$ and pH. pH: (○) 2, (●) 4, (□) 6, (■) 9.5.

Other diagrams were determined for the sedimentation behaviour of HR kaolinite mixed with unaged $FeCl_3$. This clay was composed of bigger particles than HUF kaolinite, which favoured accumulation, either as pure accumulation or as mixed accumulation–flocculation sedimentation. When the mixed regime occurred, the accumulation stage lasted a longer time than with HUF kaolinite.

Previous SEM observations showed that sodium-montmorillonite was composed of thinner particles than kaolinite. Moreover, the montmorillonite particles were partly curled. The sedimentation diagram of 0.5% by mass montmorillonite suspensions mixed with unaged $FeCl_3$ is reported in Fig. 6a, from a previous work [11]. The same figure (Fig. 6b) also shows the diagram for 1% sodium-montmorillonite suspensions mixed with aged $FeCl_3$. The diagram for 1% montmorillonite suspensions mixed with hydroxoferric particles is shown in Fig. 7a. These three diagrams are relatively similar to each other. Accumulation sedimentation occurred in a limited field of conditions at low iron content. Flocculation sedimentation occurred for all other conditions.

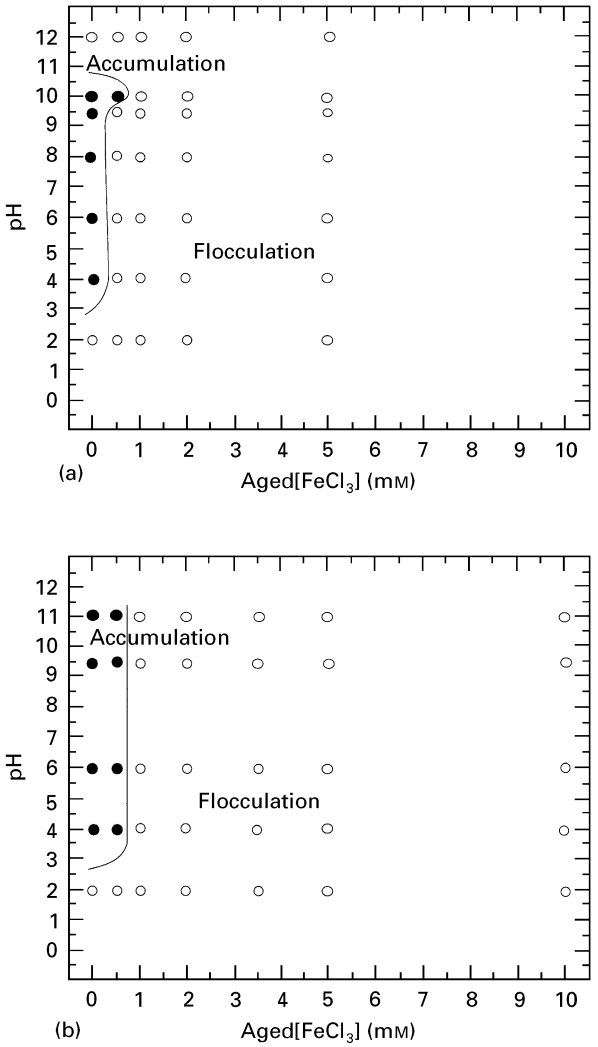

Figure 6 Diagrams of the sedimentation behaviour of (a) 0.5% sodium-montmorillonite suspensions mixed with unaged $FeCl_3$, after Zou and Pierre [11]; (b) 1% montmorillonite suspensions mixed with aged $FeCl_3$. (●) Accumulation, (○) flocculation sedimentation.

3.2. Zeta potential of clay particles

The dependence of zeta potential on pH, for sodium-kaolinite which was only treated by the method of Schofield and Samson, sodium-kaolinite treated with $Na_4P_2O_7$ and sodium-montmorillonite, are reported in Fig. 8. As stated by Schofield and Samson [4], the data on sodium-kaolinite treated according to their method are consistent with the existence of positive electric charges on the edges and negative charges on the faces of the kaolinite particles. Our data indicate an isoelectric point (i.e.p.) at pH $\approx$ 3.7, close to the known zero point of charge (z.p.c.) at pH $\approx$ 4.2. On the other hand, for sodium-kaolinite treated with $Na_4P_2O_7$, which was the only kaolinite used in the present study, the zeta potential is negative at all pH. This is consistent with the existence of negative charges only on both the edges and the faces, at all pH, before mixing with iron additives. This is also in agreement with previous statements according to which phosphate anions are responsible for these negative charges and they do not easily desorb [7]. As Fig. 8 shows, sodium-montmorillonite essentially behaves as sodium-kaolinite treated with $Na_4P_2O_7$.

For the kaolinite used in this study, that is, initially treated with $Na_4P_2O_7$, the experimental zeta potential increased algebraically with the concentration of aged $FeCl_3$, at all pH, as reported in Fig. 9a. At pH ≤ 6, the zeta potential even became positive at high $FeCl_3$ concentration. From these experimental zeta potentials, it was possible to derive a diagram composed of three fields, as a function of pH and unaged $FeCl_3$ concentration. These three fields were determined according to the absolute values of the zeta potential, in order to get the best fit with the diagrams established from the observed sedimentation behaviour (Fig. 3a). By trial and error, for the best fit, one field corresponded to data points where the zeta potential absolute value was $|\zeta| < 10$ mV. A second field corresponded to data points where $|\zeta| > 15$ mV. The third field corresponded to data points such that 10 mV $\leq |\zeta| \leq 15$ mV. This diagram is shown in Fig. 3b,

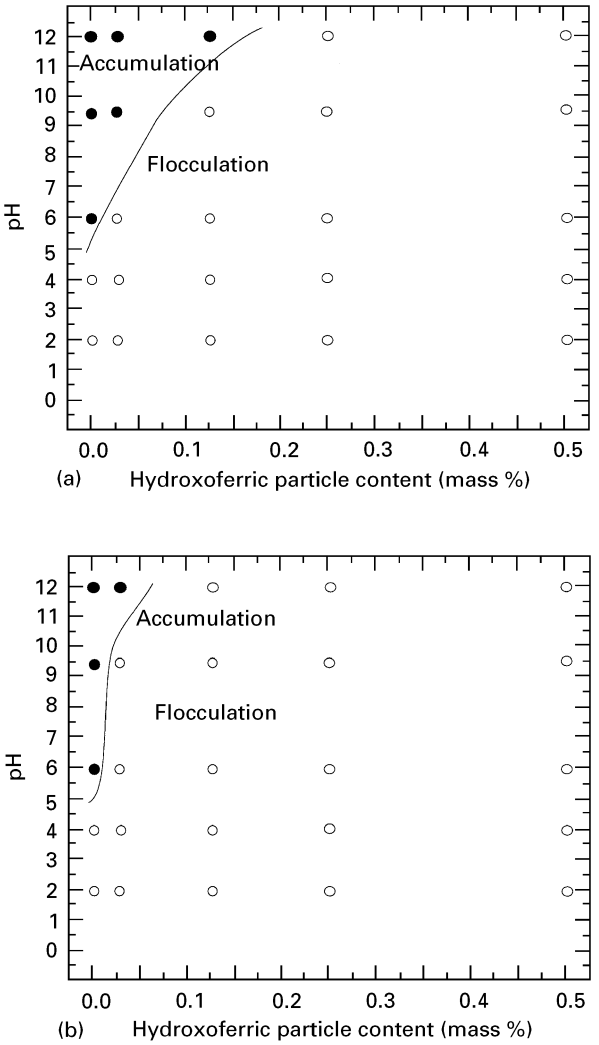

Figure 7 Diagrams of the sedimentation behaviour of 1% sodium-montmorillonite suspensions mixed with hydroxoferric particles. (a) Experimental observations: (●) accumulation, (○) flocculation sedimentation. (b) Predictions from the measured zeta potential, ζ. (○) $|\zeta| < 22$ mV, (●) $|\zeta| > 22$ mV.

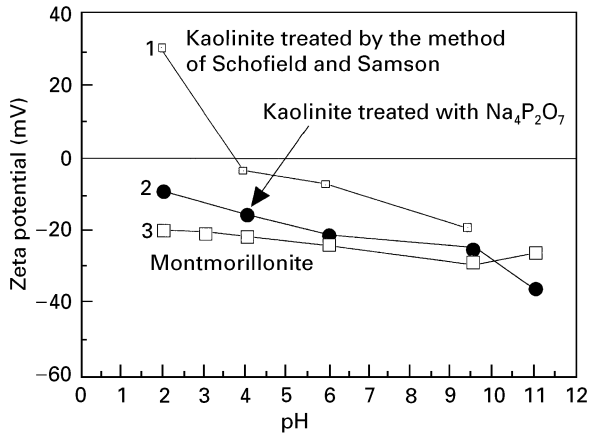

Figure 8 Relationship between the pH and the zeta potential of sodium-kaolinite and sodium-montmorillonite.

where it can be compared with the diagram from the experimental sedimentation behaviour (Fig. 3a). The two diagrams are similar to each other. Hence the sedimentation behaviour can be predicted

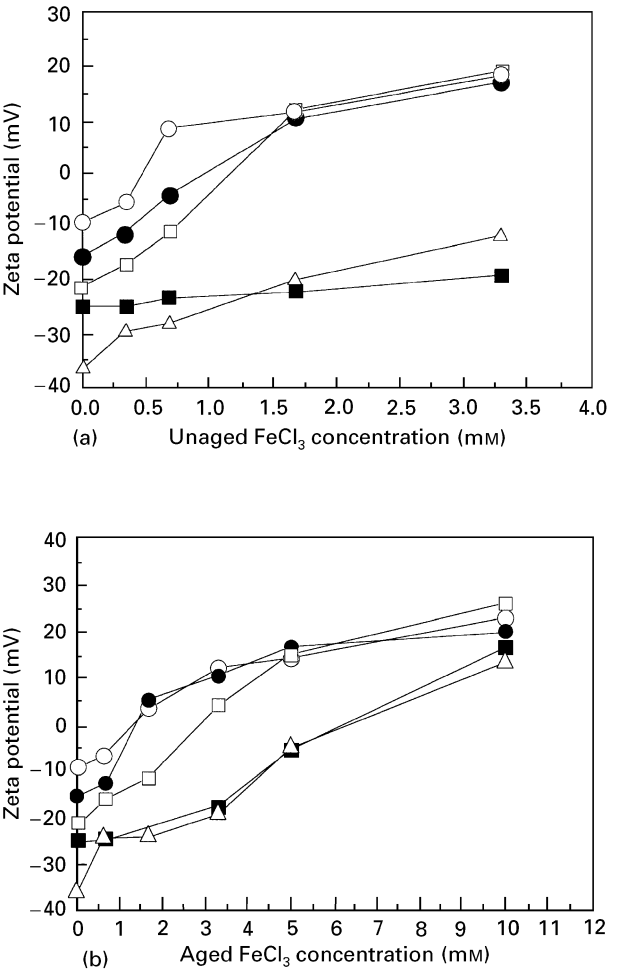

Figure 9 Variation of the zeta potential with the concentration of $FeCl_3$ at different pH values in 0.5% (by mass) kaolinite suspensions treated with $Na_4P_2O_7$: (a) unaged $FeCl_3$, pH (○) 2, (●) 4, (□) 6, (■) 9.5, (△) 11; (b) aged $FeCl_3$, pH (○) 2, (●) 4, (□) 6, (■) 9.4, (△) 11.

from the measured zeta potential. In practice, flocculation–sedimentation occurred when $|\zeta| < 10$ mV, accumulation–sedimentation occurred when $|\zeta| > 15$ mV, and mixed flocculation–accumulation sedimentation occurred when $10 \text{ mV} \leq |\zeta| \leq 15$ mV.

The zeta potential of kaolinite particles mixed with different concentrations of aged $FeCl_3$ at different pH, are reported in Fig. 9b. By comparison with Fig. 9a, the zeta potential increased from negative to positive values at all pH, with the aged $FeCl_3$ concentration. These zeta potential data were also used to build a diagram to predict the sedimentation behaviour of clay suspensions. This diagram is reported in Fig. 4b where it can be compared with the diagram from the experimental sedimentation behaviour (Fig. 4a). For the same limiting values of $|\zeta|$ as in Fig. 3b, the agreement between the predictions from the zeta potentials and the experimental sedimentation behaviour, is not as good as with unaged $FeCl_3$ (Fig. 3). However, this agreement can still be considered as being reasonable.

Similarly, the zeta potential of montmorillonite particles as a function of the hydroxoferric particles content in a suspension, at different pH, is reported in Fig. 10. The general evolution was similar to the evolution in the case of kaolinite mixed with aged $FeCl_3$. However, the magnitude of the effect was

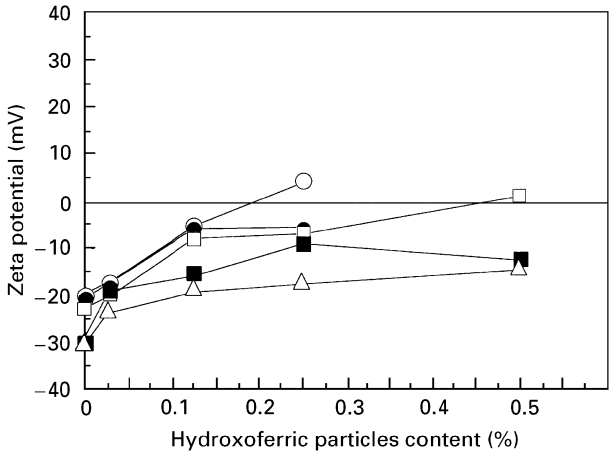

Figure 10 Zeta potential of montmorillonite particles as a function of the hydroxoferric particle content in the suspensions, and at different pH: (○) 2, (●) 4, (□) 6, (■) 9.4, (△) 12.

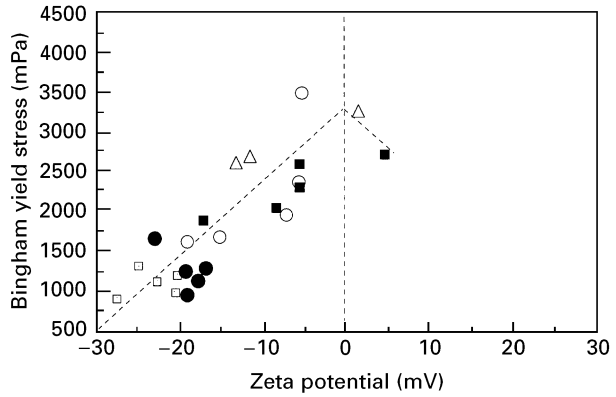

Figure 11 Relationship between the zeta potential and the Bingham yield stress in mixed montmorillonite–hydroxoferric particles suspensions (% by mass): (□) 0, (●) 0.025, (○) 0.125, (■) 0.250, (△) 0.500.

lower. In practice, this zeta potential was generally negative. Its absolute value decreased as the pH and the hydroxoferric particles content in the suspension increased. The sign of this zeta potential was only reversed and it became slightly positive for hydroxoferric particle contents of 0.25% and 0.5% (by mass), respectively, at pH = 2 and 6. The data at pH = 2 and 4, with a hydroxoferric solid content of 0.5% (by mass) could not be obtained, because flocculation of the montmorillonite suspensions occurred rapidly after addition of the hydroxoferric particles. As in the case kaolinite, a diagram was drawn to predict the sedimentation behaviour according to the value of $|\zeta|$. This is shown in Fig. 7b where it can be compared with the data from the observed sedimentation behaviour (Fig. 7a). A reasonable agreement could be reached by choosing a border value $|\zeta| = 22$ mV, to separate flocculation sedimentation from accumulation sedimentation.

The Bingham yield stress which we measured in these mixed montmorillonite–hydroxoferric particles suspensions, strongly correlated with the absolute magnitude of $|\zeta|$. The corresponding data reported in Fig. 11 indicate that, overall, the Bingham yield stress increased as $|\zeta|$ decreased.

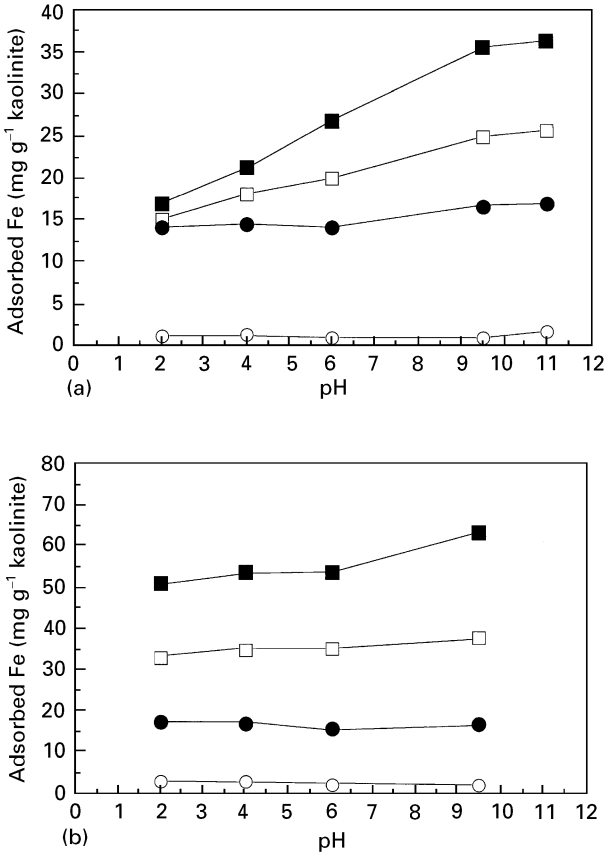

Figure 12 Amount of iron absorbed on kaolinite particles, at different pH: (a) from unaged $FeCl_3$ (mM), (○) 0.33, (●) 1.65, (□) 3.3, (■) 10; (b) from aged $FeCl_3$ (mM), (○) 0.33, (●) 1.65, (□) 3.3, (■) 10.

3.3. Other characterizations of iron-containing deposits on clay particles

Previous data showed that iron additives played an important role in modifying the zeta potential $|\zeta|$ of clay particles, and in controlling their aggregation. It was desirable to evaluate to what extent these iron additives absorbed or deposited on the surface of the clay particles. From the data on the concentration of iron which remained in the liquid of the kaolinite suspensions after 24 h sedimentation, determined by atomic absorption, it was possible to calculate the amounts of iron which were absorbed on the kaolinite particles. The results from these calculations, for unaged or aged $FeCl_3$, are reported in Fig. 12. It appears that the amount of iron adsorbed on kaolinite particles increased with the initial iron concentration, both with unaged and aged $FeCl_3$. It also increased significantly with the pH, for initial unaged $FeCl_3$ concentrations of 3.3 and 10 mM (Fig. 12a). On the other hand, the pH had a very moderate influence in the case of aged $FeCl_3$ (Fig. 12b).

The previous results obtained by atomic absorption analysis of the liquid in the clay suspensions, were consistent with TEM observations of the surface of kaolinite particles mixed with unaged $FeCl_3$. As shown in Fig. 13a, small spherical particles were deposited on the surface the clay particles, and in some places, these small spheres eventually merged to cover the kaolinite particles with a thin film. EDX analysis of the small spherical particles showed they were composed of an iron compound (Fig. 13b).

As indicated previously, a fine suspension formed in the aged $FeCl_3$ solutions before mixing in the clay suspensions. The particles in these suspensions formed various agglomerates after separation by centrifugation and drying. A powder X-ray diffraction analysis of these aggregates showed they were mostly composed of akaganéite FeOOH, mixed with other iron compounds such as haematite Fe_2O_3 (Fig. 14a). The approximate atomic composition according to EDX analysis in the SEM, was [Fe] ≈36 at%, [Cl] ≈60 at%, [O] ≈ 4 at%.

The deposits made from hydroxoferric particles were observed in the TEM in the case of montmorillonite suspensions. These hydroxoferric particles had

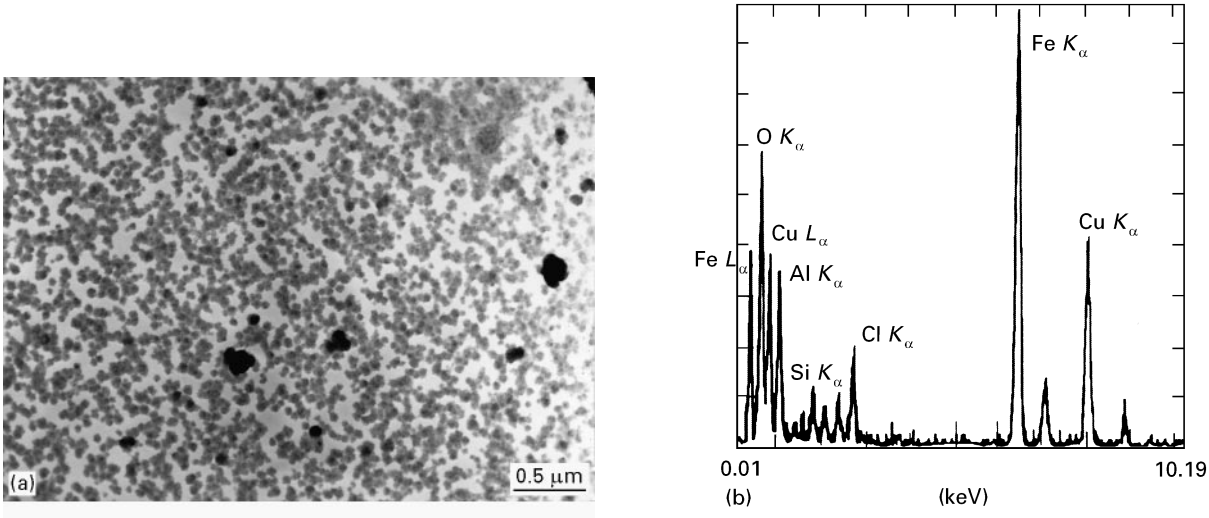

Figure 13 (a) Transmission electron micrograph of the iron material deposited on kaolinite particles, in sediments made with 10 mM unaged $FeCl_3$ at pH 9.5; (b) EDX analysis of the small spherical iron particles.

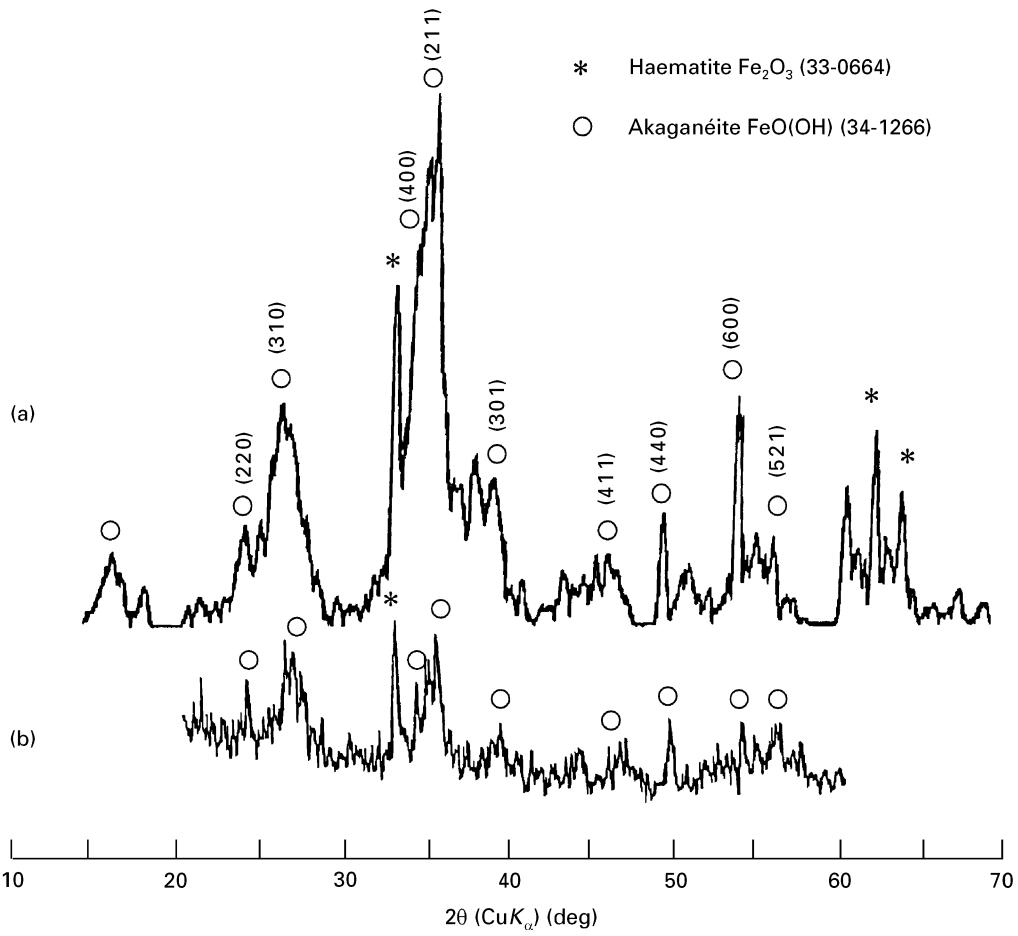

Figure 14 X-ray diffraction patterns (CuK_α, nickel-filtered) of the precipitates (a) from an aged $FeCl_3$ solution, (b) from hydroxoferric particles.

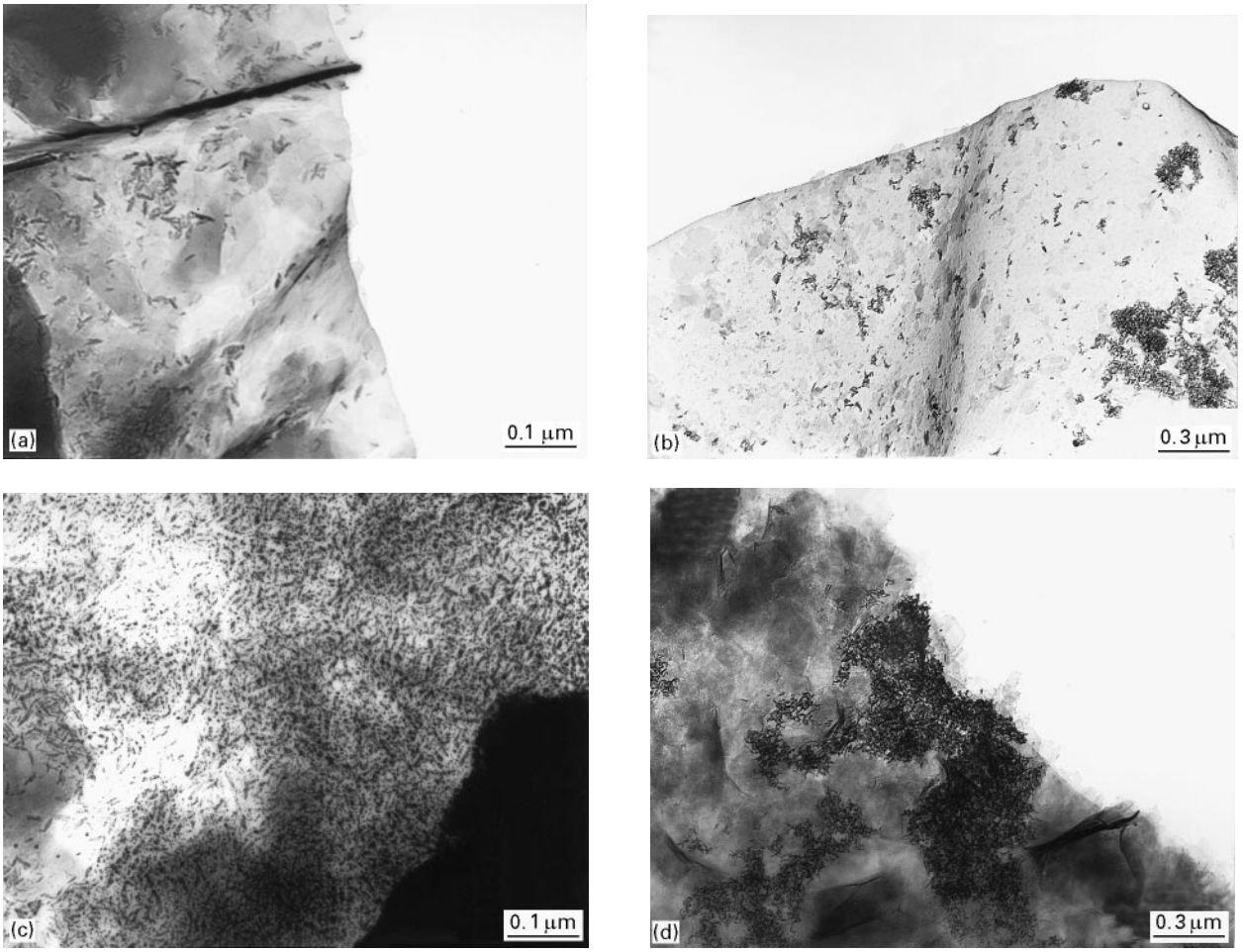

Figure 15 Transmission electron micrographs of the hydroxoferric particles deposited on montmorillonite particles, in sediments made from 1% sodium montmorillonite suspensions mixed with (a) 0.125% (by mass) of hydroxoferric particles, at pH = 2, (b) 0.125% by mass of hydroxoferric particles, at pH = 9.5, (c, d) 0.5% (by mass) of hydroxoferric particles, at pH = 2.

a characteristic which was termed "pepper-like" by Ohtsubo *et al.* [8] (Fig. 15). The X-ray diffraction patterns showed they were mostly composed of akaganéite β-FeOOH (Fig. 14b), in agreement with Ohtsubo *et al.* [8]. No obvious differences were observed in the packing pattern of these akaganéite particles on the face of the montmorillonite particles, in relation to the distance from the edge of a particle (Fig. 15). At low hydroxoferric particle content (0.125 mass %), these particles tended to form some aggregates on the faces of the montmorillonite particles. At a higher hydroxoferric particles content (0.5 mass %), a more uniform coverage of the montmorillonite particles occurred.

The influence of hydroxoferric particles on montmorillonite suspensions is well illustrated by the rheology of these suspensions. An example of a flow curve is shown in Fig. 16a. The Bingham yield stress was determined for an increasing shear rate and the data are reported, as a function of pH, in Fig. 16b. As the hydroxoferric particles content increased up to 0.5% (by mass), a stronger Bingham yield stress developed near pH = 6, that is, close to the zero point of charge (z.p.c.) of the various hydroxoferric minerals [12]. The Bingham yield stress decreased at low pH values (i.e. pH 4 and 2) far from the z.p.c. of hydroxoferric particles. At a lower hydroxoferric particle content, the yield stress was a complex function of the electrostatic

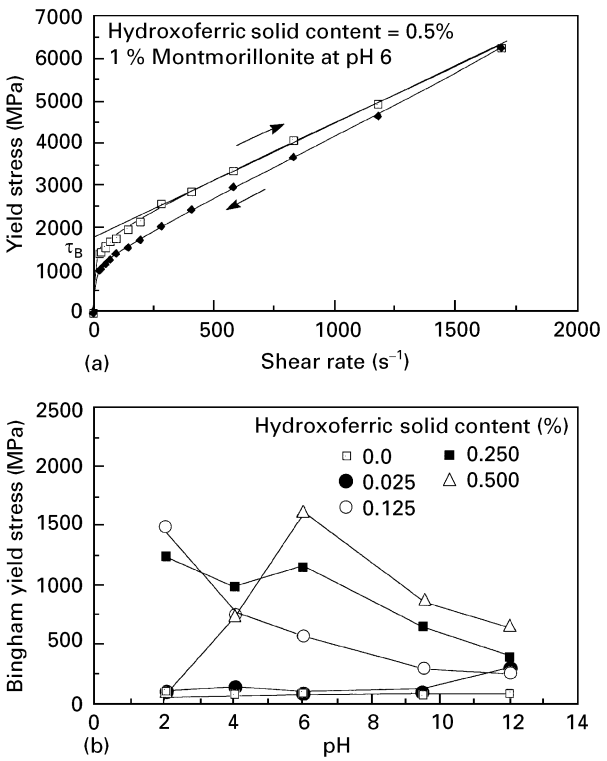

Figure 16 (a) Typical flow curve of a 1% (by mass) sodium montmorillonite suspension mixed with 0.5% (by mass) of hydroxoferric particles at pH = 6; (b) Bingham yield stress τ_B as a function of the pH, for 1% sodium-montmorillonite suspensions mixed with different hydroxoferric particles proportions.

properties of both these hydroxoferric particles and the clay particles.

4. Discussion

According to the scanning electron micrographs of kaolinite and montmorillonite sediments mixed with aluminium or iron electrolytes, obtained after supercritical-drying with CO_2 and reported in previous studies [1, 13], the packing of clay particles was more dense in the accumulated sediments than in the flocculated sediments. In the flocculated sediments, fractal flocs had formed, while a uniform packing occurred in the accumulated sediments.

From the present data on zeta potential sedimentation, diagrams very similar to the actual sedimentation diagrams could be derived. Those diagrams built from the zeta potential only depended on the absolute value of this zeta potential. A comparison of the two types of diagrams, shows that accumulation corresponded to a high absolute value of the zeta potential, i.e. $|\zeta| > 15$ mV for kaolinite and $|\zeta| > 22$ mV for montmorillonite. In such conditions, the repulsion between clay particles was high, so that these particles settled individually under gravity. Hence, a sediment was formed by random accumulation of clay particles.

On the other hand, flocculation of the clay particles corresponded to a lower absolute magnitude of the zeta potential, i.e. $|\zeta| < 10$ mV for kaolinite $|\zeta| < 22$ mV for montmorillonite. Under such conditions, the electrostatic repulsion between clay particles was lower than previously, so that these particles could aggregate in open flocs. These flocs joined to each other in order to form a single flocculated sediment. Hence, flocculation sedimentation occurred. Because kaolinite particles were thicker than montmorillonite particles, according to the scanning electron micrographs, mixed accumulation–flocculation occurred at intermediate values of the zeta potential, i.e. for $10 \text{ mV} < |\zeta| < 15$ mV, with kaolinite.

Overall, it can be concluded that the flocculation and sedimentation of clay particles, when the initial clay particles carry negative charges on both their edges and faces, is in agreement with the electrostatic stabilization theory. That is, the type of sedimentation behaviour can be predicted from the value of $|\zeta|$.

Another problem is to relate the value of $|\zeta|$ to the nature and concentration of iron additives. Although this was not the objective of the present study, some comments can be made according to the characterizations reported here.

The behaviour of Fe^{3+} electrolytes in an aqueous medium was summarized by Henry *et al.* [14] and by Livage *et al.* [15]. These electrolytes undertake complex chemical transformations through reactions of complexation, hydrolysis and condensation. Low pH (< 4) aqueous solutions are known to contain the hydroxylated monomer species $[Fe(OH_2)_6]^{3+}$ and $[Fe(OH)(OH_2)_5]^{2+}$ and the dimer species $[Fe_2(OH)_2(OH_2)_8]^{4+}$. The compound lepidocrocite γ-FeO(OH) precipitates at room temperature. Intermediate pH solutions ($4 < \text{pH} < 6$) are known to contain the monomer species $[Fe(OH)_2(OH_2)_4]^{+}$ at room temperature. Such monomers condense to polycations which have the mean composition $[Fe_4O_3(OH)_4]_n^{2n+}$ with $n = 25$. Small spheres about 2–4 nm diameter grow from these polycations and they are responsible for giving a brown–red colour to the colloidal solution. Upon ageing, or if a base is added to the solution, these polycations aggregate so as to form either β-FeO(OH) also known as akaganéite, or α-FeO(OH) needles also known as goethite. The product which is formed depends on the nature of the anions. In turn, these FeO(OH) compounds can induce the phenomenon of gelation. At high pH (> 6), the main monomeric species which is found in solution is $[Fe(OH)_3(OH_2)_3]^0$. From this monomer, α-FeO(OH) precipitates at $\text{pH} > 10$. The anions from the Fe^{3+} electrolytes participate in the complexation of these iron species and they may change the nature of the solid products which precipitate. As an example, chloride anions are known to favour the formation of the intermediate product $Fe(OH)_{2.7}Cl_{0.3}$ in the range $1.8 < \text{pH} < 3.1$, from which β-FeO(OH) needles precipitate [16].

Overall, the present analysis of iron deposits by X-ray diffraction, TEM and EDX, are consistent with the behaviour of iron electrolytes in solution, as summarized above. Akaganéite spindle particles were the main iron products, as well as small spherical iron compound particles with unaged $FeCl_3$ solutions.

The Fe^{3+} hydrolysis complexes which remained in solution acted as counterions, in the electrical double layer of negatively charged clay particles. This is consistent with the fact that flocculation occurred by adding Fe^{3+} electrolytes, which compressed the electrical double layer surrounding the clay particles, both with kaolinite (Figs 3 and 4) and montmorillonite (Figs 6 and 7). On the other hand, when the iron content was too high, the electrical double was even more compressed, so that dense clay aggregates, instead of open flocs, were formed, and accumulation of dense aggregates occurred with kaolinite (Figs 3 and 4). The fact that dense aggregation for a higher iron content was not observed with montmorillonite, could be explained by a different nature of the faces of montmorillonite and kaolinite particles. First, the kaolinite particles were very flat, and most importantly the montmorillonite particles were curled. Secondly, these surfaces can react differently to adsorb the iron complexes from the solution, which addresses a second role of iron in the present results.

The hydrolysis products from the Fe^{3+} electrolytes, as well as the hydroxoferric particles, strongly interacted with clay. A first interaction, as suggested by Thomas and Swoboda [17], is that some Fe^{3+} cationic complexes may have exchanged for Na^{+} in the clay. A second more important interaction, as shown by Blackmore [9], is that these Fe^{3+} hydrolysis products can deposit on the clay particles and establish strong links between them. Rengasamy and Oades [18, 19] used the techniques of ultrafiltration and dialysis to separate the polycations from the monomers in hydrolysed Fe^{3+} nitrate solutions. They found that the polycations chemisorbed on the OH^{-} groups

of the clay particles faces. Hence they strongly modified the electric charges on these particles faces, and they eventually reverted their sign, from negative to positive. They also were responsible for the flocculation of clay. Our zeta potential data are in agreement with these reports. Iron deposits composed of small spheres, on the faces of clay particles, are shown in Fig. 13, and similar results were also reported by Oades [20].

Blackmore [9] reported that early iron hydrolysis products are necessary to establish strong bonds between clay particles. However, he also found that the strongest bonds were achieved when a mixture of early hydrolysis products and of aged gelatinous iron was added to a clay suspension. In the present study, from a comparison between the sedimentation diagrams of kaolinite mixed with unaged and aged $FeCl_3$, (Figs 3 and 4) it is apparent that the field of conditions (pH, iron concentration) where flocculation occurred, was enlarged with aged $FeCl_3$, which is consistent with the results of Blackmore.

Moreover, the difference between the sedimentation diagrams of montmorillonite with unaged $FeCl_3$, aged $FeCl_3$ and hydroxoferric particles (i.e. akaganéite particles), is minor. Hence, it can be argued that hydroxoferric particles are very important to ensure a good bonding between the clay particles. This is confirmed by the data on Bingham yield stress of montmorillonite mixed with hydroxoferric particles and the data on iron adsorbed on the clay particles from aged and unaged $FeCl_3$. The amount of iron adsorbed on the clay particles increased with the concentration of $FeCl_3$ in the suspension (Fig. 12).

The Bingham yield stress of montmorillonite sediments mixed with hydroxoferric particles shows a maximum at pH = 6 for the highest hydroxoferric content in the present study (Fig. 16b). This result is consistent with known data on the z.p.c. of hydroxoferric particles, which are in the range pH 7–9, depending on the exact mineral form [12, 21]. When the pH of a montmorillonite suspension was close to this range, it can be assumed that the hydroxoferric particles could aggregate with each other, even after being deposited on the faces of the clay particles. Hence a heterogeneous iron gel cement bonded the clay particles. On the other hand, far from the z.p.c. range of hydroxoferric particles, such as for instance at pH = 12, the upper part of a clay sediment had a more intense brown coloration than the lower part of the sediment. This observation can be interpreted by a slower flocculation kinetics of the hydroxoferric particles, by comparison with the montmorillonite particles. That is, montmorillonite flocs and hydroxoferric flocs had partly settled independently and concurrently.

Similar results were obtained by Yong and Ohtsubo [22]. However, these authors considered that the iron compounds had built an independent gel network, entrapping the clay particles. In the present study, the clay was in much higher proportion than the iron products and the scanning electron micrographs essentially showed kaolinite or montmorillonite particles, linked to each other. Hence we conclude the iron gel only ensured a linkage between the clay particles. This coating effect and the resulting linkage between clay particles is well illustrated in Fig. 11, where the data on Bingham yield stress and zeta potential are combined, for montmorillonite mixed with hydroxoferric particles.

5. Conclusion

The aggregation and sedimentation behaviour of kaolinite particles initially treated to only carry negative electric charges, and of sodium-montmorillonite, mixed with iron additives, can be explained in terms of the absolute value of their zeta potential. A high absolute value of the zeta potential leads to random accumulation of the particles. A lower absolute value of the zeta potential leads to an aggregation of the clay particles in fractal flocs. The iron additives play an important role in a floc, to modify the zeta potential of the clay potential, and to ensure a reasonable linkage between the clay particles.

References

1. J. ZOU and A. C. PIERRE, *J. Mater Sci. Lett.* **11** (1992) 664.
2. K. MA and A. C. PIERRE, *Clay Clay Mineral.* **40** (1992) 586.
3. A. C. PIERRE, K. MA and C. BARKER, *J. Mater. Sci.* **30** (1995) 2176.
4. R. K. SCHOFIELD and H. R. SAMSON, *Discuss. Farad. Soc.* **18** (1954) 135.
5. H. VAN OLPHEN, "Introduction to Clay Colloid Chemistry", 2nd Edn (Wiley, New York, 1977).
6. D. H. YAALON, *Soil Sci. Soc. Am. J.* **40** (1976) 333.
7. S. L. SWARTZEN-ALLEN and E. MATIJEVIC, *Chem. Rev.* **74** (1974) 385.
8. M. OHTSUBO, A YOSHIMURA, S. WADA and R. N. YOUNG, *Clay Clay Mineral* **39** (1991) 347.
9. A. V. BLACKMORE, *Aust. J. Soil Res.* **11** (1973) 75.
10. A. S. MICHAELS and J. C. BOLGER, *I FC Fundam.* **10** (1962) 24.
11. J. ZOU, C. BARKER and A. PIERRE, "Proceedings of the 1991 Eastern Oil Shale Symposium", edited by J. Stivers and H. L. Retcovsky (Institute for Mining and Minerals Research, University of Kentucky, Lexington, KY, 1992) pp 233–238.
12. U. SCHWERTMANN and R. M. TAYLOR, in "Minerals in Soil Enviroments", edited by J. B. Dixon and S. B. Weed (Soil Science Society of America, Madison, WI, 1989) pp. 379–427.
13. P. SMART and N. Y. TOVEY, "Electron microscopy of soils and sediments: samples" (Clarendon Press, Oxford, 1982).
14. M. HENRY, J.P. JOLIVET and J. LIVAGE, *Structure Bond.* **25** (1990) 1.
15. J. LIVAGE, M. HENRY and C. SANCHEZ, *Prog. Solid State Chem.* **18** (1988) 259.
16. W. SCHNEIDER, *Comments Inorg. Chem.* **3** (1984) 205.
17. G. W. THOMAS and A. R. SWOBODA, *Clay Clay Mineral.* **10** (1962) 321.
18. P. RENGASWAMY and J. M. OADES, *Aust. J. Soil. Res.* **15** (1977) 221.
19. *Idem*, *ibid.* **16** (1978) 53.
20. J. M. OADES, *Clay Clay Mineral.* **32** (1984) 49.
21. S. GOLDBERG and R. A. GLAUBIG, *ibid.* **35** (1987) 220.
22. R. N. YONG and M. OHTSUBO, *Appl. Clay Sci.* **2** (1987) 63.

Received 19 April
and accepted 30 October 1996